Supplementary Information

Salt-inducible kinase 3 protects tumor cells from cytotoxic T cell attack by promoting TNF-induced NF-κB activation

Antonio Sorrentino, Ayse Nur Menevse, Tillmann Michels, Valentina Volpin, Franziska Christine Durst, Julian Sax, Maria Xydia, Abir Hussein, Slava Stamova, Steffen Spörl, Nicole Heuschneider, Jasmin Mühlbauer, Katharina Marlene Jeltsch, Anchana Rathinasamy, Melanie Werner-Klein, Marco Breinig, Damian Mikietyn, Christian Kohler, Isabel Poschke, Sabrina Purr, Olivia Reidell, Catarina Martins Freire, Rienk Offringa, Claudia Gebhard, Rainer Spang, Michael Rehli, Michael Boutros, Christian Schmidl, Nisit Khandelwal, Philipp Beckhove

Supplementary Figures

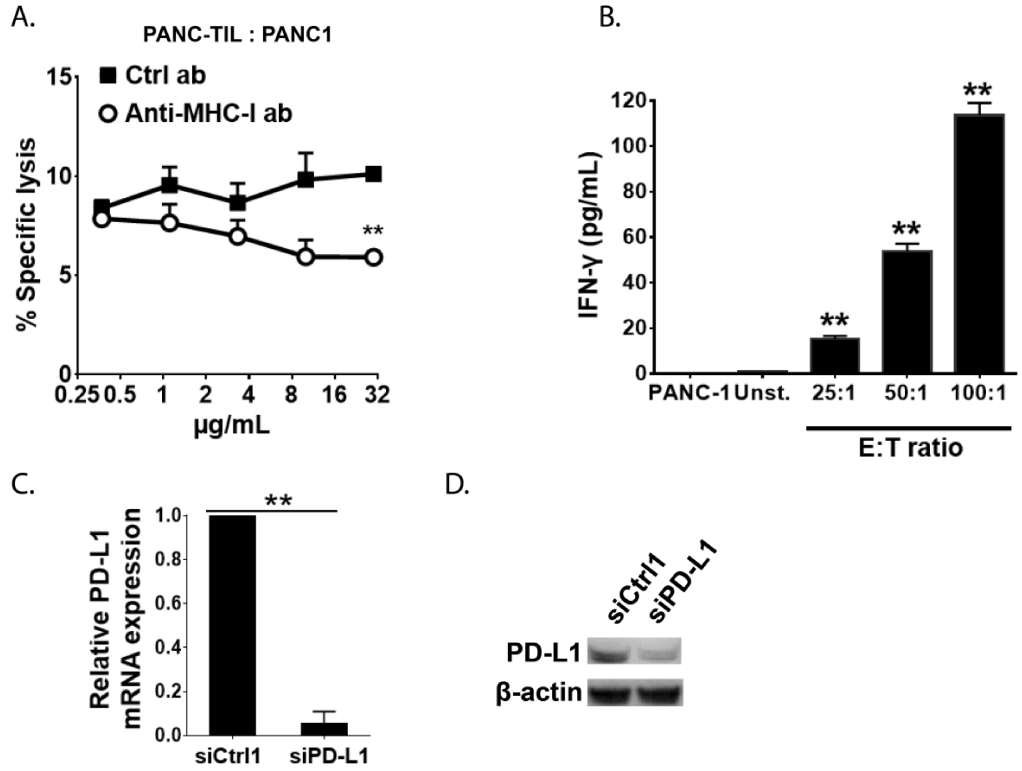

Figure S1. Setup of a HT-screening for novel immune modulators in pancreatic cancer.

(A) Chromium release assay for detection of T cell mediated cytotoxicity in the presence of the indicated concentrations of anti-MHC-I antibody (white symbols) or IgG2a isotype control (black symbols). PANC-TIL and PANC-1 cells were co-cultured for 6h at E:T ratio = 50:1. **(B)** TIL#1 and PANC-1 cells were co-cultured for 24h at the indicated E:T ratios. IFN-γ secretion was measured by ELISA: As negative control, T cells were cultured in the absence of tumor cells (Unst.). **(C)** Quantitative PCR (qPCR) analysis of PD-L1 mRNA expression in PANC-1 cells after siRNA transfection. Results are presented in terms of fold change after normalizing to β-actin. **(D)** Western blot analysis for the detection of PD-L1 protein in PANC-1 cells 72h after siRNA transfection. Graph shows representative data of at least two independent experiments. Graph shows mean +/- SEM. P-values were calculated using two-tailed student´s t-test. * $p < 0.05$, **$p<0.01$.

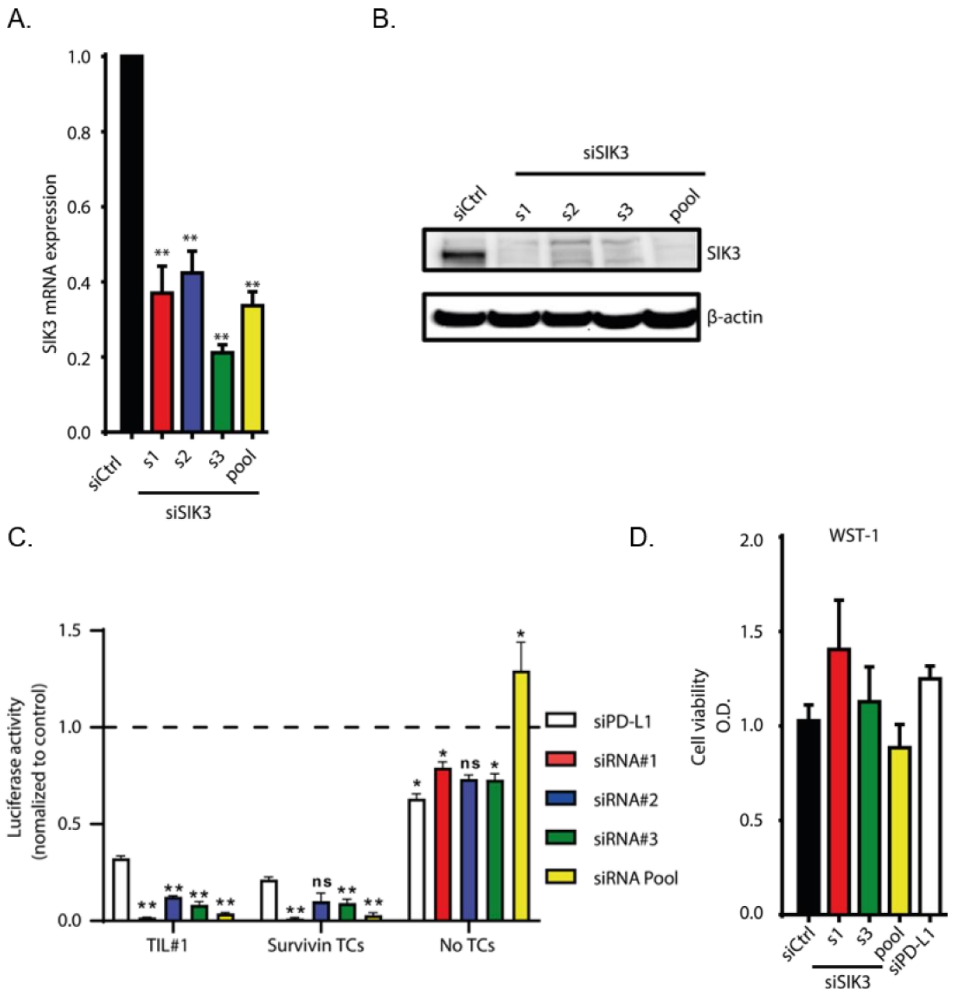

Figure S2. Assessment of SIK3-specific siRNAs' efficiency and cell viability.

(A) PANC-1-luc cells were transfected either with single (s#) or pooled (pool) siRNA sequences targeting SIK3. Scramble siRNA was used as control (siCtrl). After 72h, mRNA expression was evaluated using qPCR. Data were normalized to GAPDH. **(B)** Western blot analysis for knockdown efficiency of SIK3 using SIK3-targeting siRNAs. siRNA transfection in PANC-1-luc cells was performed as in (A). **(C)** Relative to Figure 2A. SIK3 knockdown induces stronger T cell mediated killing than PD-L1 knockdown. Unpaired t-test was conducted comparing each individual siRNA targeting SIK3 against PD-L1 knockdown, for each treatment. **(D)** Effect of SIK3-specific siRNA sequences on tumor cell viability assessed by WST-1 assay. PANC-1 cells were transfected with indicated siRNAs for 72h. Data were normalized to siCtrl. (A and C) Cumulative data of three independent experiments. Bars show mean +/- SEM values. p-values were calculated using two-tailed student´s t-test. * $p < 0.05$, ** $p < 0.01$.

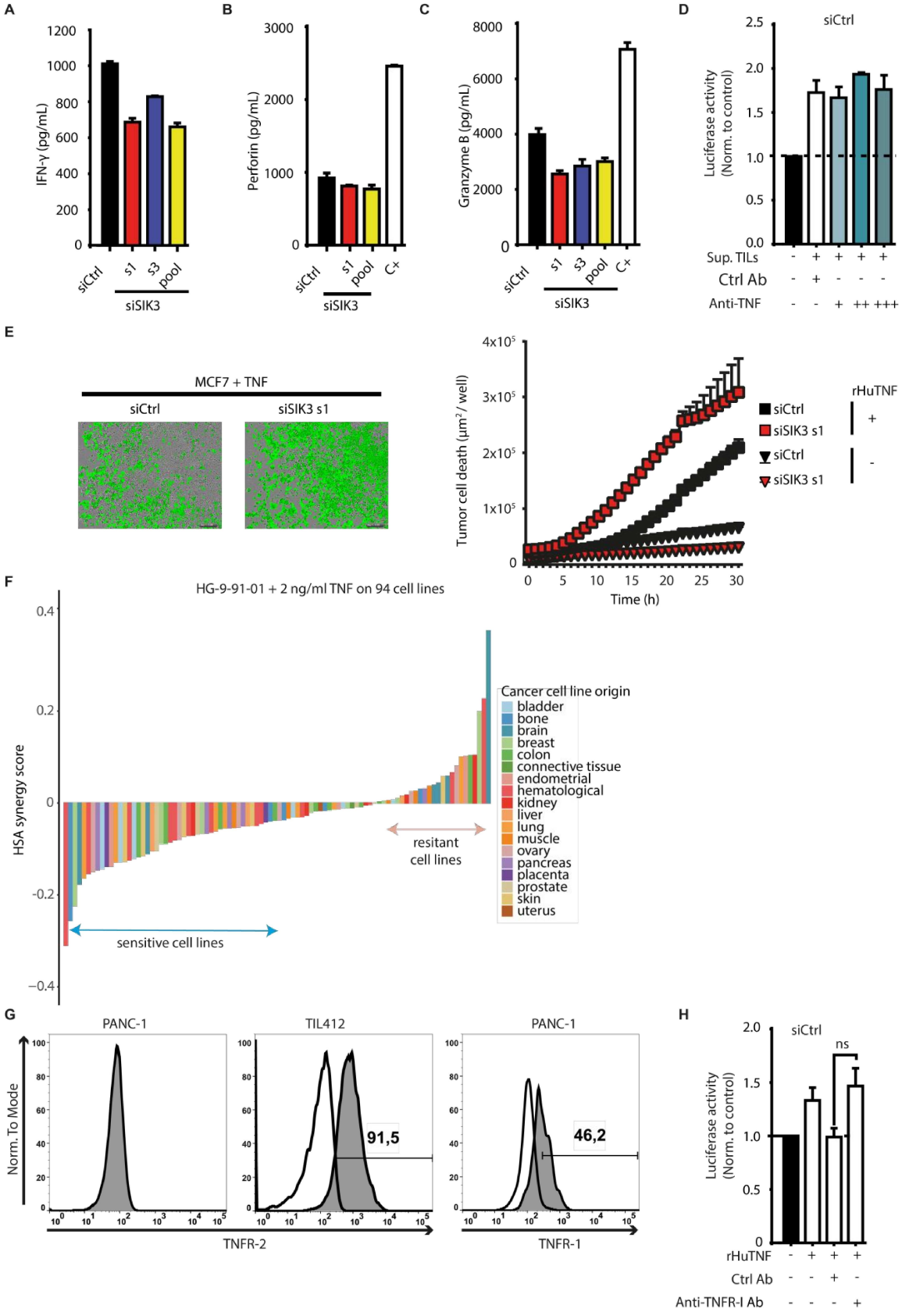
A
IFN-γ (pg/mL)
siCtrl
s1
s3
pool
siSIK3
B
Perforin (pg/mL)
C+
C
Granzyme B (pg/mL)
D
siCtrl
Luciferase activity (Norm. to control)
Sup. TILs
Ctrl Ab
Anti-TNF
E
MCF7 + TNF
siSIK3 s1
Tumor cell death (µm² / well)
Time (h)
rHuTNF
F
HG-9-91-01 + 2 ng/ml TNF on 94 cell lines
HSA synergy score
resitant cell lines
sensitive cell lines
Cancer cell line origin
bladder
bone
brain
breast
colon
connective tissue
endometrial
hematological
kidney
liver
lung
muscle
ovary
pancreas
placenta
prostate
skin
uterus
G
PANC-1
TIL412
Norm. To Mode
91,5
46,2
TNFR-2
TNFR-1
H
ns
rHuTNF
Ctrl Ab
Anti-TNFR-I Ab

Figure S3. SIK3 regulates tumor cell sensitivity to TNF.

(A) IFN-γ ELISA. PANC-1 cells were transfected with the indicated SIK3-specific siRNAs (s1, s3, pool) or scrambled siRNA (siCtrl) for 72h. Afterwards, survivin-specific TCs were added (E:T = 5:1) and after 20h INF- γ secretion was measured in co-culture supernatants. Representative data of two independent experiments. **(B)** Perforin ELISA. M579 cells were transfected as in (A) and co-cultured with TIL209 (E:T = 5:1). Perforin secretion was determined in supernatants 20h after co-culture. Phorbol 12-myristate 13-acetate (PMA)/Ionomycin stimulation served as positive control (C+). Representative data of two independent experiments. **(C)** Granzyme B ELISA. PANC-1 cells were transfected as in (A) and PANC-TIL were added at E:T = 50:1. Granzyme B secretion was measured after 20h in co-culture supernatants. Representative data of two independent experiments. **(D)** Supernatant from CD3/CD28 bead-stimulated T cells was pre-incubated with 100 (+), 300 (++) or 900 (+++) ng/ml of anti-TNF neutralizing antibody for 30 min. Isotype control (Ctrl Ab) was used at concentration of 900 ng/ml. siCtrl transfected PANC-1-luc cells were subjected to the pre-treated supernatant or control medium for 24h and cytotoxicity was measured using luciferase-based killing assay. Data are presented as fold change to unstimulated control. Cumulative data of 3 independent experiments are shown. **(E).** Effect of 100 ng/ml rHuTNF treatment on the viability of MCF-7 cells that were transfected either with siCtrl or with siSIK3 s1. The graph indicates apoptotic tumor cells as determined by the area of YOYO-1+ cells (μm^2/well). **(F)** A panel of 94 human cell lines was plated for 48 h before addition of 2 ng/ml rHuTNF and 6 different concentrations of HG-9-91-01 (1 µM- 1 nM) and incubated for 120 h. Afterwards, the optical density was analyzed using the SRB method as a measure of growth. Dose-response curves were fitted to the data (non-linear regression) and the highest single agent (HSA) model was used to calculate synergy effects. Synergy and resistance to the combination of rHu TNF and HG-9-91-01 are shown in the waterfall plot. Representative data of two independent experiments. **(G)** TNFR-2 (left panel) and TNFR-1 (right panel) expression on PANC-1 cells. TIL412 were used as positive control for TNFR-2 expression. Histograms show live, single cells after staining with primary anti-TNFR-1 or anti-TNFR-2 antibodies and PE-labelled secondary antibody. White histogram: isotype control, grey histogram: anti-TNFR-1 or anti-TNFR-2 as indicated. **(H)** Effect of TNFR-1 blockade on siCtrl transfected PANC-1-luc cells after treatment with 100 ng/mL of rHuTNF as determined by luciferase intensity. Cumulative data of three independent experiments. (A-C, F) Representative data of two independent experiments. (A-D, H) Columns show mean +/- SEM. P-values were calculated using two-tailed student´s t-test. * $p < 0.05$, ** $p < 0.01$.

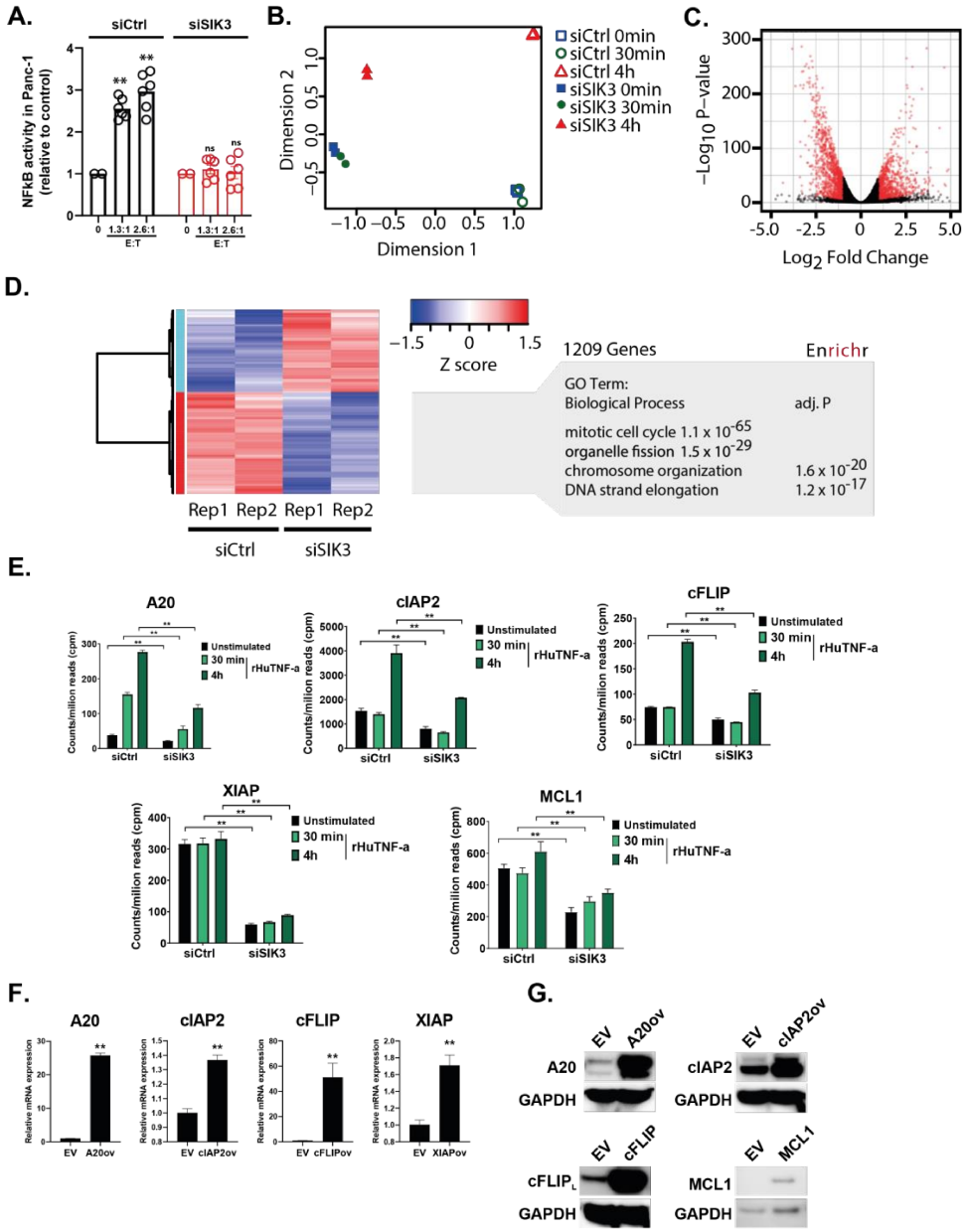

Figure S4. Effect of SIK3 knockdown on tumor cell transcription.

(A) NF-κB reporter assay**.** PANC-1 cells, carrying the luciferase gene under the control of NF-κB promoter, were transfected with the indicated siRNAs for 72h**.** Afterwards, tumor cells were co-cultured with FluT cells at the indicated E:T ratio for 12h. Tumor cells were lysed and luciferase activity was measured**. (B)** PANC-1 cells were treated with siCtrl or siSIK3 for 72h. Afterwards, TNF stimulation was applied for 30min and 4h and gene expression levels were measured using RNAseq. The multidimensional scaling (MDS) plot for replicate RNAseq data sets shows that siRNA and TNF treatment separate samples by at least 1 dimension. **(C)** Volcano Plot highlighting differentially expressed genes after SIK3 knockdown alone (fold change ≥ 2, normalized counts per million > 2, FDR ≤ .05). Red dots = genes with significant differential expression. **(D)** Two-dimensional hierarchical clustering of 2185 differentially

expressed genes (Z-score transformed, normalized counts per million; Manhattan distance, Ward method). The right panel shows representative gene enrichment analysis results for genes downregulated after SIK3 knockdown. **(E)** Related to Figure 5A: Results from the RNAseq experiment were plotted for individual genes of interest. **(F)** qPCR for the detection of overexpression level in PANC 1 cells transfected with ORF for NF-κB target genes. Data were normalized to GAPDH. **(G)** Representative WB for the assessment of protein expression in PANC-1 cells upon stable transfection with ORF for NF-κB target genes. GAPDH was used as loading control. **(F-G)** Representative data of at least two independent experiments. Columns show mean +/- SEM P-values were calculated using two-tailed student´s t-test. * $p < 0.05$, ** $p < 0.01$.

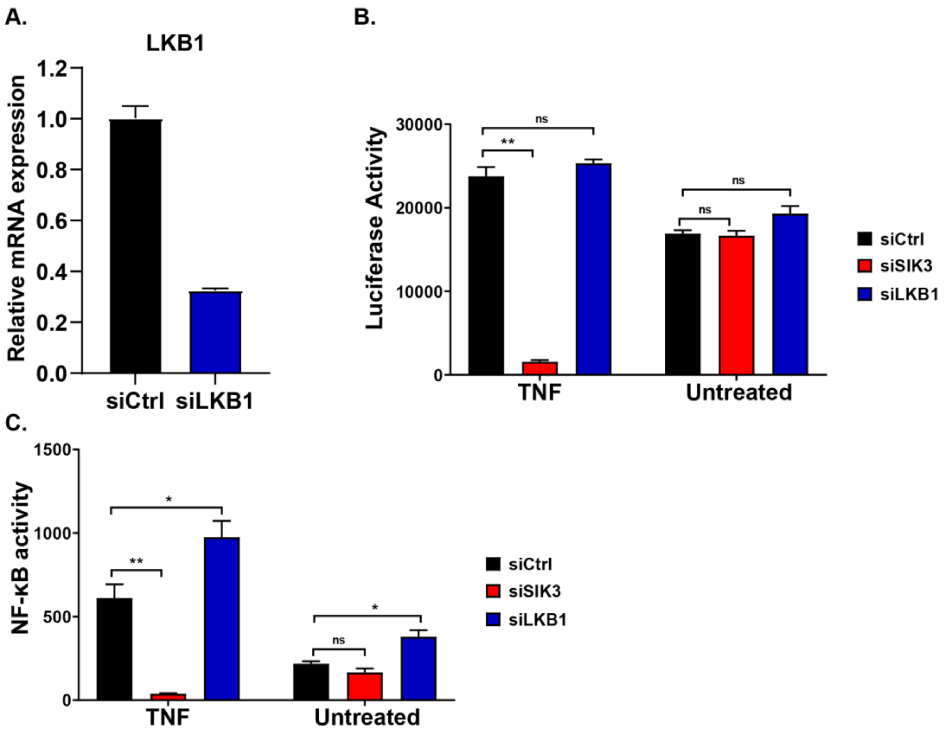

Figure S5. Role of LKB1 in regulating SIK3-mediated effects.

(A) qPCR for the detection of LKB1 mRNA levels in PANC-1 cells upon transfection of LKB1-specific siRNA. **(B)** Luciferase-based cytotoxicity assay. PANC-1 cells were transfected with the indicated siRNA, afterwards TNF stimulation (100ng/mL) was applied for 24h. Luciferase readout was performed as described in materials and methods. **(C)** NF-κB reported assay. PANC-1 cells, carrying the luciferase gene under the control of NF-κB promoter, were transfected with the indicated siRNAs for 72h**.** Afterwards, cells were stimulated with 100ng/mL of rHuTNF for 24h. Tumor cells were lysed and luciferase activity was measured. Representative data of at least two independent experiments. Columns show mean +/- SEM P-values were calculated using two-tailed student´s t-test. * $p < 0.05$, ** $p < 0.01$

Supplementary Tables

Table S2

Cell line	Normalized		Raw		Normalized		Synergy
	IC50 no TNF	IC50 + TNF	IC50 no TNF	IC50 + TNF	GI50 no TNF	GI50 + TNF	**Average HSA**
22RV1	No IC50	No IC50	No IC50	No IC50	No GI50	No GI50	-0,0080
5637	No IC50	No IC50	No IC50	No IC50	No GI50	No GI50	-0,0304
7860	8,67E-07	1,28E-06	7,78E-07	1,01E-06	8,67E-07	1,14E-06	-0,0267
A204	2,09E-07	TNF-induced apoptosis	2,18E-07	TNF-induced apoptosis	2,09E-07	No GI50	0,0365
A2780	No IC50	No IC50	No IC50	No IC50	No GI50	No GI50	0,0248
A375	No IC50	No IC50	No IC50	No IC50	No GI50	No GI50	-0,1146
A431	No IC50	No IC50	No IC50	No IC50	No GI50	No GI50	0,0575
A549	No IC50	No IC50*	No IC50	7,55E-07	No GI50	No GI50	-0,0540
A673	No IC50	No IC50	No IC50	No IC50	No GI50	No GI50	0,0253
ACHN	2,92E-07	8,74E-07	2,97E-07	2,87E-07	2,92E-07	5,75E-07	-0,0701
ASPC1	2,55E-05	No IC50	4,80E-05	No IC50	2,55E-05	No GI50	-0,0653
BT20	No IC50	TNF-induced apoptosis	No IC50	TNF-induced apoptosis	No GI50	No GI50	0,0000
BXPC3	No IC50	No IC50	No IC50	No IC50	No GI50	No GI50	-0,0499
C33A	5,87E-07	2,61E-06	1,22E-06	2,37E-05	5,87E-07	8,53E-07	-0,0125
CACO2	No IC50	No IC50	No IC50	No IC50	No GI50	No GI50	-0,0557
CAKI1	5,17E-08	6,40E-08	5,24E-08	1,29E-07	5,17E-08	1,02E-07	0,1038
CALU6	No IC50	TNF-induced apoptosis	No IC50	TNF-induced apoptosis	No GI50	No GI50	-0,1286
CASKI	No IC50	No IC50	No IC50	No IC50	No GI50	No GI50	-0,1375
CLS439	1,05E-06	5,66E-07	8,97E-07	5,71E-07	1,05E-06	4,86E-07	0,0060
COLO205	No IC50	TNF-induced apoptosis	5,12E-05	TNF-induced apoptosis	No GI50	No GI50	-0,0165
COLO678	No IC50	No IC50	No IC50	No IC50	No GI50	No GI50	-0,0080

DLD1	No IC50	No IC50	No IC50	No IC50	No GI50	No GI50	-0,0377
DU145	No IC50	No IC50	No IC50	No IC50	No GI50	No GI50	-0,1037
EFO21	No IC50	No IC50	No IC50	No IC50	No GI50	No GI50	-0,0376
EJ28	1,23E-06	7,15E-06	1,22E-06	4,72E-06	1,23E-06	2,83E-06	-0,0104
GRANTA-519	No IC50	No IC50	No IC50	1,36E-04	No GI50	No GI50	-0,0632
HCT116	No IC50	No IC50	No IC50	8,52E-07	No GI50	No GI50	-0,1168
HCT15	No IC50	No IC50	No IC50	No IC50	No GI50	No GI50	-0,0879
HEK2913	No IC50	No IC50	No IC50	No IC50	No GI50	No GI50	0,0172
HELA	2,62E-06	No IC50	2,95E-06	No IC50	2,62E-06	No GI50	0,1014
HEPG2	No IC50	No IC50	No IC50	No IC50	No GI50	No GI50	-0,1041
HL-60	No IC50	2,52E-07	1,19E-06	1,31E-07	No GI50	2,62E-07	-0,3095
HS578T	2,51E-07	6,83E-07	2,34E-07	6,15E-07	2,51E-07	3,03E-07	0,0039
HS729	No IC50	No IC50	No IC50	No IC50	No GI50	No GI50	-0,0529
HT1080	No IC50	No IC50	No IC50	No IC50	No GI50	No GI50	-0,0099
HT29	No IC50	No IC50	No IC50	No IC50	No GI50	No GI50	-0,0146
IGROV1	3,71E-07	4,97E-07	3,60E-07	5,37E-07	3,71E-07	4,90E-07	0,0802
IMR90	3,73E-08	1,62E-07	1,03E-07	3,66E-07	3,73E-08	2,06E-07	0,0998
J82	No IC50	1,11E-06	No IC50	7,32E-07	No GI50	9,61E-07	-0,1284
JAR	No IC50	4,73E-07	No IC50	3,29E-07	No GI50	4,49E-07	-0,0407
JEG3	No IC50	No IC50	No IC50	No IC50	No GI50	No GI50	-0,1376
JIMT1	No IC50	No IC50	No IC50	No IC50	No GI50	No GI50	-0,0202
K-562	2,60E-07	2,68E-07	2,58E-07	1,92E-07	2,60E-07	2,60E-07	-0,0487
KASUMI-1	No IC50	TNF-induced apoptosis	5,41E-08	TNF-induced apoptosis	5,67E-08	5,67E-08	-0,0443
L-363	2,49E-07	2,62E-07	2,41E-07	2,43E-07	2,49E-07	2,49E-07	-0,0847
LOVO	No IC50	3,87E-07	No IC50	8,61E-07	No GI50	5,29E-07	0,1035
MCF7	No IC50	No IC50	No IC50	No IC50	No GI50	2,78E-05	0,0099

MDAMB231	No IC50	No IC50	3,10E-07	2,80E-06	No GI50	7,20E-06	-0,0884
MDAMB435	No IC50	No IC50	No IC50	1,02E-07	No GI50	No GI50	-0,0728
MDAMB436	No IC50	No IC50	No IC50	No IC50	No GI50	No GI50	-0,0657
MDAMB468	No IC50	No IC50	1,00E-09	No IC50	No GI50	No GI50	-0,2239
MG63	No IC50	No IC50	No IC50	No IC50	No GI50	No GI50	-0,0393
MHHES1	1,33E-05	No IC50	1,71E-05	No IC50	1,33E-05	No GI50	-0,0155
MIAPACA2	7,76E-07	4,21E-07	7,89E-07	1,22E-07	7,76E-07	3,36E-07	-0,0537
MINO	3,93E-07	3,93E-07	3,89E-07	3,04E-07	3,93E-07	3,33E-07	-0,1240
MT3	No IC50	No IC50	MT3	No IC50	No GI50	No GI50	-0,0102
MV4-11	No IC50	TNF-induced apoptosis	5,96E-08	TNF-induced apoptosis	6,57E-08	No GI50	-0,0802
NCIH292	6,64E-07	No IC50	6,66E-07	No IC50	6,64E-07	No GI50	-0,0609
NCIH358M	No IC50	No IC50	No IC50	No IC50	No GI50	No GI50	-0,1628
NCIH460	No IC50	No IC50	No IC50	No IC50	No GI50	No GI50	-0,0301
NCIH82	No IC50	No IC50	No IC50	No IC50	No GI50	No GI50	-0,0130
OVCAR3	4,18E-07	3,86E-07	4,03E-07	1,49E-07	4,18E-07	2,20E-07	-0,1490
OVCAR4	3,00E-06	No IC50	3,80E-06	No IC50	3,00E-06	No GI50	-0,0792
PANC1	3,52E-06	7,13E-07	4,34E-06	3,80E-08	3,52E-06	5,24E-07	-0,1456
PANC1005	No IC50	No IC50	No IC50	No IC50	No GI50	No GI50	0,0305
PBMC	No IC50	No IC50	No IC50	No IC50	No GI50	No GI50	0,2263
PC3	6,84E-07	2,20E-06	7,29E-07	1,13E-06	6,84E-07	1,18E-06	-0,0673
PLCPRF5	No IC50	No IC50	No IC50	No IC50	No GI50	No GI50	0,0148
RAMOS	No IC50	No IC50	No IC50	No IC50	No GI50	No GI50	0,0659
RD	1,16E-06	1,33E-06	1,29E-06	1,25E-06	1,16E-06	9,60E-07	-0,0329
RDES	No IC50	No IC50	No IC50	No IC50	No GI50	No GI50	0,0300
SAOS2	5,51E-07	No IC50	3,68E-07	2,52E-07	5,51E-07	1,89E-07	-0,2555
SF268	1,38E-06	No IC50	1,52E-06	No IC50	1,38E-06	No GI50	0,0385
SF295	3,60E-04	No IC50	8,65E-05	1,88E-07	3,60E-04	No GI50	-0,1101

SKBR3	No IC50	No IC50	No IC50	No IC50	No GI50	No GI50	0,1990
SKHEP1	No IC50	No IC50	No IC50	No IC50	No GI50	No GI50	-0,0499
SKLMS1	No IC50	No IC50	No IC50	No IC50	No GI50	No GI50	-0,0160
SKMEL28	No IC50	No IC50	No IC50	No IC50	No GI50	No GI50	-0,0489
SKMEL5	No IC50	No IC50	No IC50	No IC50	No GI50	No GI50	-0,1276
SKNAS	2,43E-07	No IC50	2,20E-07	5,40E-08	2,43E-07	No GI50	-0,1765
SKNSH	No IC50	No IC50	No IC50	No IC50	No GI50	No GI50	0,0582
SKOV3	7,54E-07	No IC50	6,60E-07	6,45E-07	7,54E-07	7,54E-07	-0,0523
SNB75	4,03E-07	No IC50	3,36E-07	No IC50	4,03E-07	No GI50	0,0430
SU-DHL-10	No IC50	No IC50	No IC50	No IC50	No GI50	No GI50	-0,0295
SU-DHL-6	2,81E-07	No IC50	2,56E-07	4,09E-07	2,81E-07	4,50E-07	-0,0705
SW620	No IC50	No IC50	No IC50	No IC50	No GI50	No GI50	0,0020
T24	7,58E-07	5,05E-07	7,69E-07	6,56E-08	7,58E-07	7,58E-07	-0,1429
TE671	No IC50	No IC50	No IC50	No IC50	No GI50	No GI50	0,0050
THP-1	9,26E-08	8,97E-08	8,70E-08	2,84E-08	9,26E-08	7,52E-08	-0,1536
U2OS	7,91E-07	3,75E-07	7,98E-07	4,31E-07	7,91E-07	7,91E-07	-0,0364
U87MG	No IC50	No IC50	1,21E-105	No IC50	No GI50	No GI50	0,3508
UMUC3	4,73E-07	5,41E-07	4,58E-07	1,83E-07	4,73E-07	4,52E-07	-0,1205
UO31	1,82E-07	5,50E-07	1,76E-07	1,76E-07	1,82E-07	1,82E-07	-0,0037
WSU-NHL	2,67E-07	3,73E-07	2,49E-07	3,45E-07	2,67E-07	3,21E-07	-0,0029

Table S2. Raw values derived from individual tumor cell lines related to figure S3F.

Table S3

Gene	rank	regulation by SIK3	reported role in tumorigenesis	reference
ST5	1	induced	suppressor	1
ELOVL7	2	induced	promotor	2
ALCAM	3	induced	promotor	3
CD83	4	induced	n.a.	
CD40	5	induced	promotor	4
MATN2	6	induced	promotor	5
PTP4A3	7	induced	promotor	6
IFIH1	8	induced	n.a.	
CNKSR3	9	induced	suppressor	7
NFATC1	10	induced	promotor	8
ANKRD33B	11	induced	n.a.	
CFAP46	12	induced	n.a.	
FMNL3	13	induced	promotor	9
MX1	14	induced	promotor	10
CCL5	15	induced	promotor	11
STAT5A	16	induced	promotor	12
GFPT2	17	induced	promotor	13
AP1S3	18	induced	promotor	14
RIPK2	19	induced	promotor	15
SLFN5	20	induced	dual	16, 17
CD69	21	induced	n.a.	
TRAF1	22	induced	promotor	18
CLIP2	23	induced	promotor	19
CSGALNACT1	24	induced	promotor	20
CRISPLD2	25	induced	n.a.	
DRAM1	26	induced	suppressor	21
SNN	27	induced	n.a.	
GATA6	28	induced	suppressor	22
TMCC2	29	induced	n.a.	
MARCKS	30	induced	promotor	23
GLRX	31	induced	promotor	24
CCL20	32	induced	promotor	25
BTN2A2	33	induced	n.a.	
RASSF5	34	induced	suppressor	26
SEMA4C	35	induced	promotor	27
NKX3-1	36	induced	suppressor	28
RNF144A	37	induced	promotor	29
STAP2	38	induced	promotor	30
GCNT4	39	induced	n.a.	
TMEM120A	40	induced	n.a.	
DOCK10	41	induced	promotor	31
FSCN1	42	induced	promotor	32
ICAM1	43	induced	promotor	33
ALS2CL	44	induced	suppressor	34
CGN	45	induced	n.a.	
RASGEF1A	46	induced	promotor	35

BCL2L11	47	induced	n.a.	
TIAM1	48	induced	promotor	36
GABBR1	49	induced	n.a.	
SP6	50	induced	n.a.	
RFX2	51	induced	suppressor	37
XAF1	52	induced	suppressor	38
EBI3	53	induced	promotor	39
SOD2	54	induced	promotor	40
AMER1	55	induced	n.a.	
CD74	56	induced	promotor	41
DHX58	57	induced	promotor	42
RPS6KA2	58	induced	promotor	43
SPNS2	59	induced	promotor	44
RAP1GAP	60	induced	suppressor	45
BARX2	61	induced	suppressor	46
SLC15A3	62	induced	n.a.	
LRRC32	63	induced	promotor	47
TMEM231	64	induced	n.a.	
GAL	65	induced	promotor	48
CITED4	66	induced	promotor	49
CD82	67	induced	suppressor	50
SAA1	68	induced	promotor	
LAD1	69	induced	n.a.	
TTC39A	70	induced	n.a.	
CTSS	71	induced	promotor	51
CYP7B1	72	induced	n.a.	
L3MBTL4	73	induced	suppressor	52
FZD9	74	induced	dual	53
SELE	75	induced	n.a.	
TNFRSF9	76	induced	dual role	54
OAS2	77	induced	n.a.	
EGR3	78	induced	n.a.	
PDLIM4	79	induced	suppressor	55
SERPINE2	80	induced	promotor	56
MYB	81	induced	promotor	57
MGLL	82	induced	promotor	58
RFTN1	83	induced	n.a.	
KCNQ4	84	induced	promotor	59
RGS3	85	induced	n.a.	
CBFA2T3	86	induced	n.a.	
IL12A	87	induced	n.a.	
CSF2	88	induced	n.a.	
RHOV	89	induced	promotor	60
WNT4	90	induced	promotor	61
HSPA12A	91	induced	n.a.	

Table S3. Induced genes related to Fig. 5B. Genes induced by SIK3 upon TNF stimulation. Rank relates to position in Fig. 5B. Role of indicated genes in tumor promotion or suppression as reported by reference. N.a; no clear role in tumor cell intrinsic biology found.

References related to Tab S3.

1. Lichy JH, Majidi M, Elbaum J, Tsai MM. Differential expression of the human ST5 gene in HeLa-fibroblast hybrid cell lines mediated by YY1 evidence that YY1: Plays a part in tumor suppression. *Nucleic Acids Res* **24**, 4700-4708 (1996).
2. Tamura K*, et al.* Novel lipogenic enzyme ELOVL7 is involved in prostate cancer growth through saturated long-chain fatty acid metabolism. *Cancer Res* **69**, 8133-8140 (2009).
3. Kahlert C*, et al.* Increased expression of ALCAM/CD166 in pancreatic cancer is an independent prognostic marker for poor survival and early tumour relapse. *Brit J Cancer* **101**, 457-464 (2009).
4. Kim H*, et al.* Direct Interaction of CD40 on Tumor Cells with CD40L on T Cells Increases the Proliferation of Tumor Cells by Enhancing TGF-beta Production and Th17 Differentiation. *Plos One* **10**, (2015).
5. Korpos E, Deak F, Kiss I. Matrilin-2, an extracellular adaptor protein, is needed for the regeneration of muscle, nerve and other tissues. *Neural Regen Res* **10**, 866-869 (2015).
6. Stephens BJ, Han HY, Gokhale V, Von Hoff DD. PRL phosphatases as potential molecular targets in cancer. *Mol Cancer Ther* **4**, 1653-1661 (2005).
7. Nie HZ*, et al.* Mineralocorticoid receptor suppresses cancer progression and the Warburg effect by modulating the miR-338-3p-PKLR axis in hepatocellular carcinoma. *Hepatology* **62**, 1145-1159 (2015).
8. Gardberg M, Heuser VD, Koskivuo I, Koivisto M, Carpen O. FMNL2/FMNL3 formins are linked with oncogenic pathways and predict melanoma outcome. *The journal of pathology Clinical research* **2**, 41-52 (2016).
9. Baumgart S*, et al.* Inflammation-induced NFATc1-STAT3 transcription complex promotes pancreatic cancer initiation by KrasG12D. *Cancer discovery* **4**, 688-701 (2014).
10. Hastie E, Cataldi M, Moerdyk-Schauwecker MJ, Felt SA, Steuerwald N, Grdzelishvili VZ. Novel biomarkers of resistance of pancreatic cancer cells to oncolytic vesicular stomatitis virus. *Oncotarget* **7**, 61601-61618 (2016).
11. Igelmann S, Neubauer HA, Ferbeyre G. STAT3 and STAT5 Activation in Solid Cancers. *Cancers (Basel)* **11**, (2019).
12. Szymura SJ*, et al.* NF-kappa B upregulates glutamine-fructose-6-phosphate transaminase 2 to promote migration in non-small cell lung cancer. *Cell Commun Signal* **17**, (2019).
13. Sung GH, Chang H, Lee JY, Song SY, Kim HS. Pancreatic-cancer-cell-derived trefoil factor 2 impairs maturation and migration of human monocyte-derived dendritic cells in vitro. *Animal cells and systems* **22**, 368-381 (2018).
14. Zare A*, et al.* RIPK2: New Elements in Modulating Inflammatory Breast Cancer Pathogenesis (vol 10, 184, 2018). *Cancers* **10**, (2018).
15. Arslan AD*, et al.* Human SLFN5 is a transcriptional co-repressor of STAT1-mediated interferon responses and promotes the malignant phenotype in glioblastoma. *Oncogene* **36**, 6006-6019 (2017).
16. Sassano A*, et al.* Human Schlafen 5 (SLFN5) Is a Regulator of Motility and Invasiveness of Renal Cell Carcinoma Cells. *Mol Cell Biol* **35**, 2684-2698 (2015).
17. Baldwin AS. Control of oncogenesis and cancer therapy resistance by the transcription factor NF-kappaB. *The Journal of clinical investigation* **107**, 241-246 (2001).

18. Kaiser JC*, et al.* Integration of a radiation biomarker into modeling of thyroid carcinogenesis and post-Chernobyl risk assessment. *Carcinogenesis* **37**, 1152-1160 (2016).
19. Afratis N*, et al.* Glycosaminoglycans: key players in cancer cell biology and treatment. *Febs J* **279**, 1177-1197 (2012).
20. Guan JJ, Zhang XD, Sun W, Qi L, Wu JC, Qin ZH. DRAM1 regulates apoptosis through increasing protein levels and lysosomal localization of BAX. *Cell Death Dis* **6**, (2015).
21. Martinelli P*, et al.* GATA6 regulates EMT and tumour dissemination, and is a marker of response to adjuvant chemotherapy in pancreatic cancer. *Gut* **66**, 1665-1676 (2017).
22. Chen CH, Fong LWR, Yu E, Wu R, Trott JF, Weiss RH. Upregulation of MARCKS in kidney cancer and its potential as a therapeutic target. *Oncogene* **36**, 3588-3598 (2017).
23. Wang LL*, et al.* GLRX inhibition enhances the effects of geftinib in EGFR-TKI-resistant NSCLC cells through FoxM1 signaling pathway. *J Cancer Res Clin* **145**, 861-872 (2019).
24. Liu BY*, et al.* Tumor-associated macrophage-derived CCL20 enhances the growth and metastasis of pancreatic cancer. *Acta Bioch Bioph Sin* **48**, 1067-1074 (2016).
25. Zhou XH, Yang CQ, Zhang CL, Gao Y, Yuan HB, Wang C. RASSF5 inhibits growth and invasion and induces apoptosis in osteosarcoma cells through activation of MST1/LATS1 signaling. *Oncol Rep* **32**, 1505-1512 (2014).
26. Kato S*, et al.* Semaphorin 4D, a lymphocyte semaphorin, enhances tumor cell motility through binding its receptor, plexinB1, in pancreatic cancer. *Cancer Sci* **102**, 2029-2037 (2011).
27. Song LN, Silva J, Koller A, Rosenthal A, Chen EI, Gelmann EP. The Tumor Suppressor NKX3.1 Is Targeted for Degradation by DYRK1B Kinase. *Mol Cancer Res* **13**, 913-922 (2015).
28. Li BY, He LJ, Zhang XL, Liu H, Liu B. High expression of RAB38 promotes malignant progression of pancreatic cancer. *Mol Med Rep* **19**, 909-918 (2019).
29. Kitai Y*, et al.* STAP-2 protein promotes prostate cancer growth by enhancing epidermal growth factor receptor stabilization. *J Biol Chem* **292**, 19392-19399 (2017).
30. Shin S*, et al.* ERK2 regulates epithelial-to-mesenchymal plasticity through DOCK10-dependent Rac1/FoxO1 activation. *Proc Natl Acad Sci U S A* **116**, 2967-2976 (2019).
31. Chen Y*, et al.* FSCN1 is an effective marker of poor prognosis and a potential therapeutic target in human tongue squamous cell carcinoma. *Cell Death Dis* **10**, (2019).
32. Lee DJ*, et al.* Multiple tumor-suppressor genes on chromosome 3p contribute to head and neck squamous cell carcinoma tumorigenesis. *Cancer Biol Ther* **10**, 689-693 (2010).
33. Ura K, Obama K, Satoh S, Sakai Y, Nakamura Y, Furukawa Y. Enhanced RASGEF1A expression is involved in the growth and migration of intrahepatic cholangiocarcinoma. *Clinical cancer research : an official journal of the American Association for Cancer Research* **12**, 6611-6616 (2006).
34. Guo X*, et al.* Balanced Tiam1-rac1 and RhoA drives proliferation and invasion of pancreatic cancer cells. *Mol Cancer Res* **11**, 230-239 (2013).
35. Liou GY*, et al.* Mutant KRAS-induced expression of ICAM-1 in pancreatic acinar cells causes attraction of macrophages to expedite the formation of precancerous lesions. *Cancer discovery* **5**, 52-63 (2015).

36. Su JC*, et al.* RFX-1-dependent activation of SHP-1 inhibits STAT3 signaling in hepatocellular carcinoma cells. *Carcinogenesis* **35**, 2807-2814 (2014).
37. Huang J*, et al.* XAF1 as a prognostic biomarker and therapeutic target in pancreatic cancer. *Cancer Sci* **101**, 559-567 (2010).
38. Huang CB*, et al.* Tumour-derived Interleukin 35 promotes pancreatic ductal adenocarcinoma cell extravasation and metastasis by inducing ICAM1 expression. *Nat Commun* **8**, (2017).
39. He C*, et al.* SOD2 acetylation on lysine 68 promotes stem cell reprogramming in breast cancer. *Proc Natl Acad Sci U S A* **116**, 23534-23541 (2019).
40. Gold DV, Stein R, Burton J, Goldenberg DM. Enhanced expression of CD74 in gastrointestinal cancers and benign tissues. *Int J Clin Exp Patho* **4**, 1-12 (2011).
41. Ranoa DRE*, et al.* Cancer therapies activate RIG-I-like receptor pathway through endogenous non-coding RNAs. *Oncotarget* **7**, 26496-26515 (2016).
42. Milosevic N*, et al.* Synthetic lethality screen identifies RPS6KA2 as modifier of epidermal growth factor receptor activity in pancreatic cancer. *Neoplasia* **15**, 1354-1362 (2013).
43. Gu XY*, et al.* SPNS2 promotes the malignancy of colorectal cancer cells via regulating Akt and ERK pathway. *Clin Exp Pharmacol P* **46**, 861-871 (2019).
44. Zhang LZ*, et al.* Identification of a putative tumor suppressor gene Rap1GAP in pancreatic cancer. *Cancer Res* **66**, 898-906 (2006).
45. Chen H*, et al.* Downregulation of BarH-like homeobox 2 promotes cell proliferation, migration and aerobic glycolysis through Wnt/-catenin signaling, and predicts a poor prognosis in non-small cell lung carcinoma. *Thorac Cancer* **9**, 390-399 (2018).
46. Tran DQ, Andersson J, Wang R, Ramsey H, Unutmaz D, Shevach EM. GARP (LRRC32) is essential for the surface expression of latent TGF-beta on platelets and activated FOXP3(+) regulatory T cells. *P Natl Acad Sci USA* **106**, 13445-13450 (2009).
47. Chetry M*, et al.* The Role of Galectins in Tumor Progression, Treatment and Prognosis of Gynecological Cancers. *Journal of Cancer* **9**, 4742-4755 (2018).
48. Hsieh CH, Chou YT, Kuo MH, Tsai HP, Chang JL, Wu CW. A targetable HB-EGF-CITED4 axis controls oncogenesis in lung cancer. *Oncogene* **36**, 2946-2956 (2017).
49. Zhu JD*, et al.* The metastasis suppressor CD82/KAI1 regulates cell migration and invasion via inhibiting TGF-beta 1/Smad signaling in renal cell carcinoma. *Oncotarget* **8**, 51559-51568 (2017).
50. Djurec M*, et al.* Saa3 is a key mediator of the protumorigenic properties of cancer-associated fibroblasts in pancreatic tumors. *P Natl Acad Sci USA* **115**, E1147-E1156 (2018).
51. Gautam J, Bae YK, Kim JA. Up-regulation of cathepsin S expression by HSP90 and 5-HT7 receptor-dependent serotonin signaling correlates with triple negativity of human breast cancer. *Breast Cancer Res Tr* **161**, 29-40 (2017).
52. Addou-Klouche L*, et al.* Loss, mutation and deregulation of L3MBTL4 in breast cancers. *Mol Cancer* **9**, (2010).
53. Zeng CM, Chen Z, Fu L. Frizzled Receptors as Potential Therapeutic Targets in Human Cancers. *Int J Mol Sci* **19**, (2018).
54. Glorieux C, Huang P. Regulation of CD137 expression through K-Ras signaling in pancreatic cancer cells. *Cancer Commun* **39**, (2019).
55. Vanaja DK*, et al.* PDLIM4, An Actin Binding Protein, Suppresses Prostate Cancer Cell Growth. *Cancer Invest* **27**, 264-272 (2009).
56. Yang Y, Xin XK, Fu X, Xu DM. Expression pattern of human SERPINE2 in a variety of human tumors. *Oncol Lett* **15**, 4523-4530 (2018).

57. Srivastava SK, *et al.* MYB is a novel regulator of pancreatic tumour growth and metastasis. *Brit J Cancer* **113**, 1694-1703 (2015).
58. Li CF, *et al.* Transcriptomic reappraisal identifies MGLL overexpression as an unfavorable prognosticator in primary gastrointestinal stromal tumors. *Oncotarget* **7**, 49986-49997 (2016).
59. Comes N, *et al.* Involvement of potassium channels in the progression of cancer to a more malignant phenotype. *Bba-Biomembranes* **1848**, 2477-2492 (2015).
60. Haga RB, Ridley AJ. Rho GTPases: Regulation and roles in cancer cell biology. *Small GTPases* **7**, 207-221 (2016).
61. Vouyovitch CM, *et al.* WNT4 mediates the autocrine effects of growth hormone in mammary carcinoma cells. *Endocrine-related cancer* **23**, 571-585 (2016).
62. Zhang H, *et al.* LAMB3 mediates apoptotic, proliferative, invasive, and metastatic behaviors in pancreatic cancer by regulating the PI3K/Akt signaling pathway. *Cell Death Dis* **10**, (2019).
63. Li H, *et al.* C1QTNF1-AS1 regulates the occurrence and development of hepatocellular carcinoma by regulating miR-221-3p/SOCS3. *Hepatology international* **13**, 277-292 (2019).
64. Liu N, Gao F, Han Z, Xu X, Underhill CB, Zhang L. Hyaluronan synthase 3 overexpression promotes the growth of TSU prostate cancer cells. *Cancer Res* **61**, 5207-5214 (2001).

Table S4

Gene	rank	regulation by SIK3	reported role in tumorigenesis	Reference
ANGPTL4	1	repressed	suppressor	1
ID2	2	repressed	promotor	2
INTS6	3	repressed	suppressor	3
SPRY1	4	repressed	suppressor	4
TOB1	5	repressed	suppressor	5
EID3	6	repressed	suppressor	6
KCNQ1OT1	7	repressed	suppressor	7
GNAI1	8	repressed	suppressor	8
HES1	9	repressed	suppressor	9
HIST4H4	10	repressed	n.a.	
HTR1B	11	repressed	suppressor	10
MEG3	12	repressed	suppressor	11
FOXQ1	13	repressed	promotor	12
DMRTA1	14	repressed	n.a.	
SNAI1	15	repressed	promotor	13
SNORD17	16	repressed	n.a.	
GRIP1	17	repressed	n.a.	
CALCRL	18	repressed	n.a.	

Table S4. Repressed genes; related to Fig. 5B. Genes repressed by SIK3 upon TNF stimulation. Rank relates to position in Fig. 5B. Role of indicated genes in tumor promotion or suppression as reported by reference. N.a; no clear role in tumor cell intrinsic biology found.

References related to Tab S4.

1. Coma S, Amin DN, Shimizu A, Lasorella A, Iavarone A, Klagsbrun M. Id2 Promotes Tumor Cell Migration and Invasion through Transcriptional Repression of Semaphorin 3F. *Cancer Res* **70**, 3823-3832 (2010).
2. Filleur S*, et al.* INTS6/DICE1 inhibits growth of human androgen-independent prostate cancer cells by altering the cell cycle profile and Wnt signaling. *Cancer Cell Int* **9**, (2009).
3. Hidalgo-Sastre A*, et al.* Hes1 Controls Exocrine Cell Plasticity and Restricts Development of Pancreatic Ductal Adenocarcinoma in a Mouse Model. *Am J Pathol* **186**, 2934-2944 (2016).
4. Lee HS, Kundu J, Kim RN, Shin YK. Transducer of ERBB2.1 (TOB1) as a Tumor Suppressor: A Mechanistic Perspective. *Int J Mol Sci* **16**, 29815-29828 (2015).
5. Liu JY, Wu XY, Wu GN, Liu FK, Yao XQ. FOXQ1 promotes cancer metastasis by PI3K/AKT signaling regulation in colorectal carcinoma. *Am J Transl Res* **9**, 2207-+ (2017).
6. Ma L*, et al.* Long non-coding RNA MEG3 functions as a tumour suppressor and has prognostic predictive value in human pancreatic cancer. *Oncol Rep* **39**, 1132-1140 (2018).
7. Masoumi-Moghaddam S, Amini A, Morris DL. The developing story of Sprouty and cancer. *Cancer Metast Rev* **33**, 695-720 (2014).
8. Okochi-Takada E*, et al.* ANGPTL4 is a secreted tumor suppressor that inhibits angiogenesis. *Oncogene* **33**, 2273-2278 (2014).
9. Shuno Y*, et al.* Id1/Id3 Knockdown Inhibits Metastatic Potential of Pancreatic Cancer. *J Surg Res* **161**, 76-82 (2010).
10. Sun X*, et al.* Overexpression of long non-coding RNA KCNQ1OT1 is related to good prognosis via inhibiting cell proliferation in non-small cell lung cancer. *Thorac Cancer* **9**, 523-531 (2018).
11. Takai D*, et al.* Silencing of HTR1B and reduced expression of EDN1 in human lung cancers, revealed by methylation-sensitive representational difference analysis. *Oncogene* **20**, 7505-7513 (2001).
12. Yao J*, et al.* GNAI1 Suppresses Tumor Cell Migration and Invasion and is Post-Transcriptionally Regulated by Mir-320a/c/d in Hepatocellular Carcinoma. *Cancer biology & medicine* **9**, 234-241 (2012).
13. Yin T, Wang CY, Liu T, Zhao G, Zha YH, Yang M. Expression of snail in pancreatic cancer promotes metastasis and chemoresistance. *J Surg Res* **141**, 196-203 (2007).

Supplementary Material and Methods

^{51}Chromium-release assay

Tumor cells were detached and labelled with 100 µL 51Cr/106 target cells in CLM for 1 h at 37 °C. Afterwards, cells were washed with CLM and incubated with PBS-EDTA (1:20 dilution; Merck Millipore) at 37°C for 10 minutes. Tumor cells were counted and 3000 target cells per well were co-cultured with T cells in 96 well u-bottom plates at the indicated E:T

ratios for 6 h at 37°C. Plates were centrifuged and 100 µL of supernatants were collected in 96-well Luma plates (Perkin Elmer, Waltham USA). Plates were dried overnight, and radioactivity counted in the Gamma counter (Cobra counter Packard, Perkin Elmer). Spontaneous release was measured from the target cells that are incubated with medium alone, whereas maximum release was determined from the target cells incubated with 10% Triton X-100 (Merck Millipore) instead of T cells. The percent of specific lysis was calculated by using the formula given below: % Specific lysis = (experimental release-spontaneous release) / (maximum release-spontaneous release) × 100.

Influenza-specific CD8+ T cells

For the generation of influenza (Flu)-specific CD8+ T (FluT) cells, PBMCs from HLA-A*02+ healthy donors were isolated. Total CD8+ T cells were sorted from PBMCs by magnetic separation and expanded in the presence of A2-matched Flu peptide (GILGFVFTL, ProImmune, Oxford, UK) for 14 days. The autologous CD8- fraction was irradiated and used for 1 week as feeder cells, which were then substituted with irradiated T2 cells. On day 1 and day 8, 100 U/ml IL2 and 5 ng/µL IL15 were added. Cells were expanded in expansion medium composed of 50% CLM and 50% AIM-V medium. After 14 days of antigen-specific expansion, pentamer-labelled Flu-antigen specific T cells were sorted by FACS and expanded further for 14 days according to the rapid expansion protocol from Rosenberg *et al.* [1].

Western blot

Tumor cells were centrifuged and cell pellets resuspended in lysis buffer (MILLIPLEX MAP Lysis Buffer from Merck Millipore, protease inhibitor cocktail (Merck Millipore) and phosphatase inhibitor cocktail (Sigma-Aldrich)) and kept on ice for 15 min. After mixture, whole cell lysate was cleared by centrifugation (10 min, 10000g, 4 °C). For cytosolic and nuclear extraction cell pellets were resuspended in 5 cell pellet volumes ice cold Buffer A (10 mM HEPES (pH 7.9), 1.5 mM MgCl2, 10 mM KCl, 1 mM DTT, 0.1% Triton X-100 and

Protease and Phosphatase Inhibitor Cocktail). After 10 min incubation cell suspension was centrifuged (300 g, 5 min, 4°C), supernatant discarded and pellet thoroughly resuspended in two volumes of Buffer A. After a centrifugation step (8000 g, 20 min, 4°C) the supernatant was collected containing cytoplasmic proteins. The remaining pellet was lysed with 2/3 of the original pellet volume ice cold Buffer B (20 mM HEPES (pH 7.9), 1.5 mM MgCl2, 0.42 M NaCl, 0.2 mM EDTA, 1 mM DTT, 1.0% NP-40, 25% (v/v) glycerol, Protease and Phosphatase Inhibitor Cocktail). Nuclear extract was collected after 45 min incubation at 4°C using a rotator and centrifugation (16000g, 5 min, 4°C). The protein content in the lysate was measured by using Pierce BCA Protein Assay Kit (Thermo Scientific) according to manufacturer's protocol. For immunoblot analysis, 30–50 µg of total protein were denatured in NuPAGE LDS Sample Buffer (Thermo Scientific) at 70°C for 10 min and separated on the NuPAGE 4-12% Bis-Tris Gels (Thermo Scientific). Separated protein bands were transferred onto PVDF membrane (Merck Millipore) using 1X wet-transfer buffer at 400 mA for 1 h at 4°C. Membranes were blocked with 5% milk powder in TBS at room temperature (RT) for 1-2 h. For the detection of phosphorylated proteins, membranes were blocked with 5% BSA in TBS-T. Membranes were incubated overnight at 4°C with the indicated primary antibodies. The following antibodies were purchased from Cell Signaling and used at 1:1000 dilution: rabbit monoclonal anti-A20/TNFAIP3 (D13H3, Cat.#5630), rabbit monoclonal anti-c-IPA2/BIRC3 (58C7,Cat.#3130), rabbit monoclonal anti-XIAP (3B6, Cat.#2045), rabbit monoclonal anti-Bcl-xL/BCL2L1 (54H6, Cat.#2764), rabbit monoclonal anti-Mcl-1 (D2W9E, Cat.#94296), rabbit monoclonal anti-CFLAR/FLIP (D5J1E, Cat.#56343), rabbit polyclonal anti-IKKβ (L570, Cat.#2678), rabbit polyclonal anti-IKKα (Cat.#2682), rabbit monoclonal anti-phospho-IKKα/β (Ser176/180) (16A6, Cat.#2697), rabbit monoclonal anti-IκBα (44D4, Cat.#4812), rabbit monoclonal anti-phospho-IκBα (Ser32) (14D4, Cat.#2859), rabbit monoclonal anti-LKB1 (27D10, Cat.#3050), rabbit monoclonal anti-phospho-LKB1 (Ser428) (C67A3,

Cat.#3482), anti-HDAC4, anti-pHDAC4 (Ser246), anti-NF-κB and polyclonal anti-acNF-κB (Lys310) and anti-Histone H3. As housekeeper gene, mouse monoclonal anti-GAPDH (0411, Cat.#sc-47724) was purchased from Santa Cruz and used 1:200. Rabbit polyclonal anti-SIK3 was purchased from Abcam, Cat.#88495 and used 1:1000. Membranes were washed 3 times with TBS-T for 10 min and incubated 1 h at room temperature with HRP-conjugated secondary antibodies (anti-mouse and anti-rabbit, Santa Cruz, Dallas, USA) prepared in 1% milk in TBS-T or in 5% BSA in TBS-T for the detection of phosphorylated proteins. Protein bands were detected using ECL developing solution from GE Healthcare and the chemiluminescent signal was detected using the My ECL Imager (Thermo Scientific).

PCR and qPCR

Synthesized cDNA was amplified using conventional PCR. PCR samples were set up in a 25 µL volume using 2x MyTaq HS Red Mix (Bioline, Luckenwalde, Germany), 500 nM of gene-specific primer mix (Qiagen, Hilden, Germany) and 100 ng of template cDNA. The PCR program was set as follows: 95°C for 3 min, 35 cycles of a 3 repetitive steps of denaturation (95°C for 15 s), annealing (60°C for 20 s) and extension (72°C for 15 s), and a final step at 72°C for 7 min. PCR products were run on a 2% agarose gel and visualized using a UV documentation system (Konrad Benda, Wiesloch, Germany). For qPCR, 10 ng of template cDNA, 2x QuantiFast SYBR Green PCR mix (Qiagen) and 300 nM of gene-specific primer mix was used per 20 µL reaction. Reactions were run using the 7300 Real-Time PCR System (Thermo Scientific, Waltham, Massachusetts, USA). The following primers were used for cDNA detection: RT2 qPCR Primer Assay for Human MCL1 (QIAGEN PPH00397E-200); RT2 qPCR Primer Assay for Human XIAP (QIAGEN PPH00323A-200); RT² qPCR Primer Assay for Human SIK3 (QIAGEN PPH21242A-200); RT2 qPCR Primer Assay for Human BIRC3 (cIAP2) (QIAGEN PPH00326B-200); RT2 qPCR Primer Assay for Human CFLAR (QIAGEN PPH00333B-200); RT2 qPCR Primer Assay for Human TNFAIP3 (A20) (QIAGEN

PPH00063A-200). Expression of analyzed genes was normalized to the expression of β-actin (Fwd: AGAAAATCTGGCACCACACC; Rvs: GGGGTGTTGAAGGTCTCAAA) or GAPDH (QIAGEN PPH00150F-200) genes and the analysis was performed using comparative Ct method.

Gene overexpression

For SIK3 overexpression 3 x 10^5 M579 cells or 2 x 10^6 PANC-1 cells were seeded in a 6-well plate overnight at 37°C, 5% CO2. 3 µg of SIK3-overexpression plasmid (GenScript, Piscataway USA) or the empty vector (EV) control (pCDNA3.1; GenScript) were diluted in 150 µL of Opti-MEM (Thermo Scientific) in the presence of 3 µL of the plus reagent. 15 µL of Lipofectamine LTX (Thermo Scientific) was suspended in 150 µL of Opti-MEM. The DNA-containing solution was added to the liposome-containing suspension and incubated for 30 min at RT. The tumor cell medium was replaced with 1 ml of Opti-MEM and the DNA-liposome mixture was added dropwise to the tumor cells. After 24 h the tumor cell medium was replaced with normal cell culture medium. PANC-1- luc cells overexpressing the anti-apoptotic genes (A20 (NM_001270508.2), cIAP2 (NM_001165.5), cFLIP (NM_003879.7), XIAP (NM_001167.3) and MCL-1 (NM_021960.5)) were generated by stable transfection. PANC-1-luc cell line was transfected with the ORF for each gene, cloned in pcDNA3.1/Hygro(+) vectors, obtained from GenScript (Clone IDs: OHu14590, OHu18994,OHu23686, OHu20683, OHu21277 respectively), using jetOptimus (PolyPlus, cat.#. 101000051), according to manufacturer's instructions. The transfected cells were selected with 500 µg/ml Hygromycin B (Carl-Roth, cat.# 1287.2).

ELISA

siRNA-transfected PANC-1 or M579 cells were co-cultured with different T cell sources at the indicated E:T ratio for 20 h and 100 µL of supernatants were harvested for the detection of IFN γ (Human IFN-γ ELISA Set; BD OptEIA™; Heidelberg, Germany), perforin (Human Perforin

ELISA PRO kit, Mabtech, Nacka Strand, Sweden) and granzyme B (Human Granzyme B ELISA development kit; Mabtech). Experiments were performed according to the manufacturer´s instructions. PMA/Ionomycin (Merck Millipore; 50 ng/ml and 1 µg/ml final concentration respectively) stimulation was used as a positive control. Absorbance was measured at $\lambda = 450$ nm, taking $\lambda = 570$ nm as reference wavelength using a microplate reader (TECAN, Männedorf, Switzerland).

Flow cytometry

For flow cytometry experiments, live cells were distinguished by using Live/Dead Fixable Yellow dead Cell Stain (Life Technologies) followed by blocking with kiovig (human plasma-derived immunoglobulin, Baxter, Deerfield, Illinois, USA) at a concentration of 100 µg/ml in FACS buffer (PBS, 2% FCS) for 15 min at 4°C. Samples were washed in FACS buffer and incubated with either fluorophore-conjugated primary antibody or isotype control (anti-PD1; Biolegend, San Diego, USA 1:20, anti-TIM-3 and anti-LAG3; both R&D Systems, Miniapolis, USA 1:20). Cells were acquired with the FACS Canto II cell analyzer machine (BD). For indirect flow cytometry (TNFR-I (Hycult biotech) or TNFR-II (Acris antibodies) stainings) samples were incubated with the primary antibody and subsequently stained with phycoerythrin (PE)-conjugated secondary antibody 1:4000 (Jackson Immuno) for 20 min on ice in the dark. For assessing tumor cell proliferation, 50000 M579 tumor cells or PANC-1 tumor cells labeled with 0.5µM CFSE (eBioscience) were plated in 6 well plates and left to adhere. After 3-4 h, TIL209 or TIL412 (in CLM medium) were added to M579 cells at varying E:T ratios. Similarly, TILs or FluT cells (in CLM medium) were added to PANC-1 tumor cells. PANC-1 cells were previously pulsed with Flu peptide for 2h in the wells where FluT cells were to be added. 24 h later, cells were disrupted using trypsin EDTA (Lonza) and live cells were distinguished by using the Live/Dead Fixable Yellow dead Cell Stain followed by blocking with kiovig and stained for EpCAM or the corresponding isotype control antibody

(Biolegend) for 20 min at 4°C. Cells were then fixed and permeabilized using fixation and permeabilization concentrate and diluent from eBioscience for 20 min at 4 °C followed by intracellular staining for Ki67 (BD Biosciences) in 1x permeabilization solution (eBioscience) for 20 min at 4 °C. Acquisition of cells were performed using the BD LSRII, and data analysis was done with FlowJo V10 software. EpCAM positive PANC-1 cells were analyzed for Ki67 expression. CFSE-stained M579 cells were analysed for Ki67 expression.

TNF-α catch assay

1 x 10^6 TILs cells were co-cultured with 1 x 10^6 PANC-1 WT cells (E:T = 1:1) in a 12-well plate. Alternatively, TILs were polyclonally stimulated with PHA (5 µg/ml final concentration; Merck Millipore). Unstimulated T cells served as negative control. After 12h incubation, T cells were collected and stained with the TNF secretion assay (catch assay) kit (Miltenyi biotech, Bergisch Gladbach, Germany) according to manufacturer´s instructions. Briefly, TILs were collected and incubated with the cytokine catch reagent for 5 min on ice. Afterwards, warm medium was added and cells were incubated for 1 h at 37°C, 5% CO2. Catch reagent was washed out and the cytokine detection antibody (PE-conjugated) was added together with anti-CD3, anti-CD4 and anti-CD8 antibodies in the presence of Live/Dead Fixable Yellow dead Cell Stain (1:1000). After 20 min incubation on ice in the dark TILs were washed twice and measured via FACS.

NF-κB reporter assay

TNF-induced NF-κB activity in PANC-1 cells was measured using NF-κB-dependent luciferase activity. NF-κB reporter PANC-1 cells (carrying the luciferase gene under the control of NF-κB promoter) were seeded in 96 or 384-well plates for 24 h (experiment with inhibitors) or 72h (experiment with siRNAs) Afterwards, cells were treated with different concentrations of the SIK3 inhibitor HG-9-91-01 for one hour before addition of 10 ng/ml rHu

TNF for 7h at 37°C and 5% CO_2. For siRNA-based assays, 100 ng/mL of rHuTNF was used for 24h. Afterwards, cells were lysed, and luciferase activity was measured.

pHDAC4 MSD assay

HDAC4 phosphorylation levels in PANC-1 cells were measured using a Meso Scale Discovery assay. PANC-1 cells (6 x 1010^4) were seeded in a 96-well plate overnight and subsequently treated with 10 ng/mL rHu TNF and different concentrations of the SIK3 inhibitor HG-9-91-01 for 3 h at 37°C and 5% CO_2. Whole cell lysates were generated using RIPA lysis buffer (Thermo Scientific) and incubated on GAM plates coated with anti-total HDAC4 antibody (Abcam ab12171) overnight at 4 °C. Afterwards, phosphorylated HDAC4 was detected using the pHDAC4 antibody (CST#3443). ECL signal was measured using an MSD reader.

Luminex assays

TNF was quantified using BioPlex ProHuman Chemokine TNFa Set (Bio-Rad) according to the manufacturer´s instructions. Samples were measured using the MAGPIX luminex instrument (Merck Millipore). For detection of intracellular analytes involved in apoptosis PANC-1 cells were stimulated with rHuTNF (100 ng/ml) for 2h or 4 h, lysed and 20 µg of protein lysates were used for detection of phosphorylated Akt (Ser473), JNK (Thr183/Tyr185), Bad (Ser112), Bcl-2 (Ser70), p53 (Ser46) or cleaved Caspase-8 (Asp384) and Caspase-9 (Asp315) by MILLIPLEX MAP Early Phase Apoptosis 7-plex-kit (Millipore) according to the manufacturer´s instructions. Samples were measured using the MAGPIX luminex instrument (Merck Millipore).

Real-time live cell imaging

Transfected tumor cells were challenged either with T cells or with 100 ng/ml of rHuTNF. Alternatively, 1 x 10^5 M579 were seeded in a 96-well plate flat overnight and subsequently challenged with TIL209 (5:1). In some experiments, TILs were labelled with Cell Trace Far Red (Cell Trace Proliferation Kit from Thermo Scientific) prior to co-culture. All reactions

were conducted in the presence of the YOYO-1 dye (Thermo Scientific), (1:1000). Plates were incubated in the Incucyte ZOOM live-cell imager (Essen Bioscience, Welwyn Garden City, UK) at 37°C and 5% CO_2 and images were acquired at the indicated time points. Data were analyzed with the Incucyte ZOOM 2016A software (Essen Bioscience) by creating a top-hat filter-based mask for the calculation the area of YOYO-1 incorporating cells (dead cells).

WST-1 assay

The WST-1 Cell Proliferation Assay (Roche, Basel, Switzerland) was used to measure viability of PANC-1. In short, PANC-1 cells were reverse transfected and 10 µL of the WST-1 reagent was added to each well and incubated for 1h at 37°C, 5% CO_2. The absorbance was measured at $\lambda = 450$ nm versus $\lambda = 650$ nm reference by using the Spark microplate reader (TECAN). In some cases, reverse transfected cells were stimulated with the supernatant of polyclonally stimulated T cells for 24h before the addition of the WST-1 reagent.

TNF sensitization assay

TNF sensitization was measured in a screening of 94 different solid cancer cell lines (Oncolead, Munich, Germany). In short, cell lines were seeded (varying media, seeding density btw. 500 – 7000 cells/well) in a 96-well plate for 48 h at 37°C and 5% CO_2. Afterwards, cells were treated with different concentrations of HG-9-91-01 (1, 4, 16, 64, 250 and 1000 nM) and 2 ng/ml rHu TNF for 120 h at 37°C and 5% CO_2. Cytotoxicity was measured using sulforhodamine B as described before. Plate normalization was performed on all values by subtracting the background value (average optical density of wells with medium but without cells). Dose response curves were calculated using non-linear curve fitting. IC_{50} and growth inhibition of 50 % (GI_{50}) were calculated and log10-transformed. Synergy between HG-9-91-01 and TNF treatment was calculated by the highest single agent model.

ELISA

The NF-κB p50/p65 EZ-TFA Transcription Factor assay kit (Merck Millipore) was used to measure the nuclear translocation of the p65 subunit of the NF-κB complex. Briefly, PANC-1 WT or Hela cells were reverse transfected with desired siRNAs. Tumor cells were then stimulated either with 100 ng/ml of rHuTNF or with CLM for 15 or 30 min. Alternatively, PANC-1 WT cells were transfected with SIK3 overexpressing plasmid or EV (GenScript). The cytosolic protein fraction was separated from the nuclear protein fraction according to the manufacturer`s protocol. The protein concentration of nuclear fractions was determined using the BCA kit (Thermo Scientific) according to the manufacturer's protocol. 4.5 µg of nuclear lysate were added in each well of the pre-coated NF-κB (p65 subunit) ELISA 96-well plate. The assay was performed according to the manufacturer´s instructions and absorbance was measured at $\lambda = 450$ nm, taking $\lambda = 570$ nm as reference wavelength using the Spark microplate reader (TECAN).

Pre-processing and analysis of ATAC-seq data

ATAC-seq reads were trimmed using Skewer [2] and aligned to the hg38 assembly of the human genome using Bowtie2 [3] with the '-very-sensitive' parameter and a maximum fragment length of 2,000. Duplicate and unpaired reads were removed using the sambamba[4] 'markdup' command, and reads with mapping quality >30 and alignment to the nuclear genome were kept. All downstream analyses were performed on these filtered reads. For visualization purposes only, coverage files from filtered bam files were produced using bedtools genomeCoverageBed command [5]. Each position was normalized by dividing to the total library size and multiplying by 10^6, followed by conversion to a bigwig using the bedGraphToBigWig command from the UCSC genome browser tools.

Bioinformatics analysis of chromatin accessibility data

Peak calling was performed using HOMER [6] with the following approach: Two different peak sets were called, once we used the options "-style factor -fragmentLength 150 -size 350 -minDist 350 -L 4 -fdr 0.001 -tbp 1" parameters, to identify highly robust small regions of open chromatin, and in a second approach we used the parameters "-region -fragmentLength 150 -size 150 -minDist 350 -L 4 -fdr 0.001 -tbp 1" to identify larger regions of open chromatin. The two peak sets were then intersected using the bedtools intersect command with the "-u" option to create the peak set that was used for downstream analysis. For the analysis of sample sets we always created a consensus region set by merging the called peaks from all involved samples using bedtools, and we quantified the accessibility of each region in each sample by counting the number of reads from the filtered BAM file that overlapped each region. Peaks overlapping blacklisted features as defined by the ENCODE project [7] were discarded.

To normalize the chromatin accessibility signal across samples, we performed quantile normalization followed by GC content normalization by regression using the cqn R package [8]. Principal component analysis was performed with the scikit-learn library (sklearn.decomposition.PCA) applied to the chromatin accessibility values for the merged peaks across all samples in the respective sample sets. DESeq2 [9] was used on the raw count values for each sample and regulatory element to identify differential chromatin accessibility between samples. Significant regions were defined as having an FDR-corrected p-value below 0.05, an absolute $\log_2$fold change above 1, and a mean accessibility equal or greater than 10.

Motif enrichment analysis was done using HOMER [6] with the function findMotifsGenome using "-size 500 -len 8,10,12 -h" parameters. Motifs from analyses were combined to a merged motif file and filtered for redundant motifs using HOMER's compareMotifs function with the parameters "-reduceThresh 0.6 -matchThresh 10 -info 0.6 -pvalue 1e-25" and were compared to the vertebrate known motifs from the HOMER database. The enrichment of this reduced

motif set was then calculated in the peaks of the respective comparisons using the annotatePeaks function. Histograms of reads around transcription factor binding motifs were generated using HOMER by centering the peaks of interest on the investigated motifs using the annotatePeaks function, followed by counting reads from individual experiments at single base pair resolution in a radius of 1000 bp (or 150 bp) around the peak centers using the annotatePeaks function with the parameters "-hist -fragLength 1". For these histograms, all reads aligning to the + strand were offset by +4 bp, and all reads aligning to the – strand were offset −5 bp to represent the center of the transposon binding event as described previously[10]. Shifted reads were then converted in tag directories using HOMER, merged for replicate samples, and used as input for the annotatePeaks function.

Peaks were assigned to their nearest TSS using the HOMER promoter annotation. Enrichment of genes associated with regulatory elements (annotated with the nearest transcription start site) was performed thorough the Enrichr API [11] for the KEGG 2016 dataset.

References to Supplementary Materials and Methods

1. Jin J, et al. Simplified method of the growth of human tumor infiltrating lymphocytes in gas-permeable flasks to numbers needed for patient treatment. J Immunother **35**, 283-292 (2012).

2. Jiang H, Lei R, Ding SW, Zhu S. Skewer: a fast and accurate adapter trimmer for next-generation sequencing paired-end reads. BMC Bioinformatics **15**, 182 (2014).

3. Langmead B, Salzberg SL. Fast gapped-read alignment with Bowtie 2. Nat Methods **9**, 357-359 (2012).

4. Tarasov A, Vilella AJ, Cuppen E, Nijman IJ, Prins P. Sambamba: fast processing of NGS alignment formats. Bioinformatics **31**, 2032-2034 (2015).

5. Quinlan AR, Hall IM. BEDTools: a flexible suite of utilities for comparing genomic features. Bioinformatics **26**, 841-842 (2010).

6. Heinz S, et al. Simple combinations of lineage-determining transcription factors prime cis-regulatory elements required for macrophage and B cell identities. Mol Cell **38**, 576-589 (2010).

7. Consortium EP. An integrated encyclopedia of DNA elements in the human genome. Nature **489**, 57-74 (2012).

8. Hansen KD, Irizarry RA, Wu Z. Removing technical variability in RNA-seq data using conditional quantile normalization. Biostatistics **13**, 204-216 (2012).

9. Love MI, Huber W, Anders S. Moderated estimation of fold change and dispersion for RNA-seq data with DESeq2. Genome Biol **15**, 550 (2014).

10. Buenrostro JD, Giresi PG, Zaba LC, Chang HY, Greenleaf WJ. Transposition of native chromatin for fast and sensitive epigenomic profiling of open chromatin, DNA-binding proteins and nucleosome position. Nat Methods **10**, 1213-1218 (2013).

11. Kuleshov MV, et al. Enrichr: a comprehensive gene set enrichment analysis web server 2016 update. Nucleic Acids Res **44**, W90-97 (2016).